Iranian Journal of Astronomy and Astrophysics
Vol. 12, No. 2, Spring 2025, 111–125
©Available online at http://ijaa.du.ac.ir
DOI: 10.22128/ijaa.2025.3030.1223
Online ISSN: 2383–403X

Iranian Journal of Astronomy and Astrophysics

Research Paper

Boundary-Driven Kelvin-Helmholtz Waves in a Space Magnetized Plasma

Mahboub Hosseinpour
Faculty of Physics, University of Tabriz, Tabriz, P.O.Box:16471, Iran;
E-mail: hosseinpour@tabrizu.ac.ir

Received: 26 August 2025; **Accepted:** 20 September 2025; **Published:** 23 Septembere 2025

Abstract. Kelvin-Helmholtz instability (KHI) is a shear flow-driven instability that imposes important changes in the macroscopic dynamics of some magnetized plasmas such as the solar corona, astrophysical jets, and Earth's magnetopause. Using two-dimensional magnetohydrodynamic (MHD) simulations, the externally driven KHI is studied in a compressible plasma with a uniform magnetic field parallel to the direction of flow streaming. We show that the perpendicular perturbation of either plasma velocity or magnetic field on the fluid boundary in the form of a single localized pulse or a sinusoidal wave or a superposition of multiple sinusoidal waves with random wavelengths and amplitudes results in the excitation and the fast growth of KHI on the interface layer. It is found that as the wavelength of sinusoidal perturbation is smaller or the amplitude is larger, the KHI becomes faster. However, in the fully nonlinear regime, the dynamics of KHI becomes independent of the type or the magnitude of boundary perturbation. Moreover, it is shown that when the boundary is disturbed by a single highly localized pulse of plasma velocity, the formation location of KH vortices on the interface layer is irregular. The KHI will then develop throughout the interface layer. The externally forced KHI is more effective in space and astrophysical plasmas when the internal perturbations are absent or very weak on the interface layer, or the initially weak shear flow is unable to trigger the KHI sufficiently. In these environments, the boundaries are highly likely to be disturbed continuously or intermittently by external fluid motions.

Keywords: Kelvin-Helmholtz Instability, Externally driven, MHD Simulation, Space plasma, Boundary perturbation

1 Introduction

The relative motion of two plasma fluids separated by a thin interface layer can be unstable to the Kelvin–Helmholtz instability (KHI; [1–3]). Rolling up of the interface and subsequent vortex formation is a typical signature of the KHI. The KH dynamics then develops into a nonlinear stage involving large-size vortices, and eventually, the turbulent motions appear where vortices merge and monster vortices emerge. Strong gradients of plasma and magnetic pressures and magnetic tension force define KHI's primary and fundamental dynamics.

KHI is a well-known viable mechanism for momentum and energy exchange and transport between two different plasma fluids. It is important for the understanding of space and

astrophysical phenomena involving a sheared plasma flow, such as the interaction between the solar wind and planetary magnetospheres and ionospheres [4–9] and the structure of cometary tails [10]. KHI has also been applied in MHD models of pulsar magnetospheres and extragalactic radio jets [11–14]. KHI has been extensively studied in the low solar corona. For instance, ripples at the prominence surface [15], billows on the flank of coronal mass ejecta [16–18] and traveling fluctuations at the boundaries of magnetic structures [19] have been attributed to the KH instability.

Until now, magnetized KHI has been extensively studied analytically, numerically, experimentally, and observationally by taking into account different physics, effects, and various ranges of main parameters such as compressibility, viscosity, resistivity or with the presence of non-uniform mass density or temperature (e.g. [20] and references therein). In previous numerical studies, KHI was initiated by applying a small perturbation on the interface layer separating two fluids. As the instability develops, associated oscillations propagate away from the interface layer and change the plasma dynamics almost throughout the fluids. On the other hand, the external boundaries of a plasma can be disturbed continuously or intermittently (with low or high frequency) by the perpendicular perturbations of plasma flow, pressure, or magnetic field. Consequently, the perturbations propagate in the fluids and eventually affect the interface layer, where the KHI occurs. In particular, when the spatial sizes are finite, the external disturbance becomes more effective. Moreover, when the plasma is dilute (i.e., low density), the propagation of external perturbations in the form of magnetoacoustic waves towards the interface layer is faster. Therefore, the interface layer can be affected quickly. In addition, the effect of boundary perturbation in driving KHI becomes important when the initial shear flow is substantially weak or the internal perturbation on the interface layer is extremely poor to excite the KHI. This type of KHI being driven externally (forced KHI), has not already been discussed in the relevant literature. Therefore, it is interesting to study this problem here.

Considering externally driven instabilities, several works have studied the issue of forced magnetic reconnection, known as the "Taylor problem" which its onset is due to the boundary disturbance of a highly conductive plasma embedded in a magnetic field that changes its direction in a narrow region [21–23]. The external perturbations propagate towards the current sheet. As a result, magnetic field lines cut and reconnect to each other continuously within a current sheet due to the presence of some non-ideal MHD effects such as the plasma resistivity, electron inertia, or electron pressure gradient. On the other hand, the phenomenon of magnetic reconnection can be initiated within the current sheet by applying an appropriate perturbation on the magnetic field or plasma resistivity within the current sheet. This type of magnetic reconnection is known as the "spontaneous magnetic reconnection".

In this study, similar to the "Taylor problem" in the forced magnetic reconnection [21], we investigate the onset and growth of KHI on the interface layer with a shear flow due to perturbations of the plasma velocity on either the up or down boundary. Boundary perturbation assumed in our study is a sinusoidal wave with a specified wavelength and amplitude or a superposition of multi-waves with random wavelengths and amplitudes. Moreover, the boundary perturbation can be in the form of a single localized pulse. The consequent dynamics of KHI will be discussed by considering each of these three types of boundary perturbation. To do so, the rest of the paper is structured as follows: in the next section, the simulation setup and initial model are presented. The results are given in Section 3, followed by a summary and conclusion in Section 4.

2 Simulation Setup

Two-dimensional MHD simulations use the PLUTO code, a publicly available numerical code for astrophysical plasma simulations developed at the University of Turin [24]. PLUTO solves conservative partial differential MHD equations, equation (1). It is an Eulerian, finite volume, shock-capturing code based on high-order Godunov methods providing several integration algorithms, Riemann solvers, time-stepping methods, and interpolation schemes. The set of single-fluid ideal MHD equations in the conservative form to be solved numerically is

$$\begin{aligned} \frac{\partial \rho}{\partial t} + \nabla.(\rho \mathbf{V}) &= 0, \\ \frac{\partial \mathbf{m}}{\partial t} + \nabla.[\mathbf{m}\mathbf{V} - \mathbf{B}\mathbf{B} + \mathbf{I}(P + \frac{\mathbf{B}^2}{2})] &= 0, \\ \frac{\partial \mathbf{B}}{\partial t} + \nabla \times \mathbf{E} &= 0, \\ \frac{\partial E_t}{\partial t} + \nabla.[(\frac{\rho \mathbf{V}^2}{2} + \rho e + P)\mathbf{V} + \mathbf{E} \times \mathbf{B}] &= 0, \end{aligned} \tag{1}$$

where the Ohm's law defines the electric field, $\mathbf{E} = -\mathbf{V} \times \mathbf{B}$ with the electric current density $\mathbf{J} = \nabla \times \mathbf{B}$. Here, the permeability constant is set to one, $\mu_0 = 1$. For the sake of simplicity, we ignore the effect of plasma resistivity by setting $\eta = 0$. Actually, including the resistivity term in the generalized Ohm's law, mainly affects on the evolution of magnetic field, and its effect on the dynamics of KHI is less significant, in particular, in small values of resistivity, which is the relevant case in space and astrophysical plasmas. Furthermore, $E_t = \rho e + \frac{\mathbf{m}^2}{2\rho} + \frac{\mathbf{B}^2}{2}$ is the total energy density with e, ρ, $\mathbf{m}$ and $\mathbf{B}$ being the internal energy density, mass density, momentum density, $\mathbf{m} = \rho \mathbf{V}$, and magnetic field respectively. Finally, $\mathbf{V}$ and $\mathbf{I}$ are the bulk velocity of plasma and the unitary tensor. An ideal equation of state provides the closure for MHD equations in the form $\rho e = P/(\Gamma - 1)$, where P and Γ are thermal pressure and the constant ratio of specific heats. The divergence-zero constraint for the magnetic field, $\nabla.\mathbf{B} = 0.$, is being checked by the code at every time-step of integration of equations.

To set up the initial conditions for the growth of KHI, the mass density is given as $\rho(y) = (\rho_1 + \rho_2)/2 + ((\rho_2 - \rho_1)/2)\, tanh(y/\Delta)$ with a narrow half width $\Delta = 0.01$, $\rho_1 = 1.0$ and $\rho_2 = 0.5$. Meanwhile, as an essential condition, the plasma velocity hyperbolic tangent profile is defined by $\mathbf{V}(y) = V_0\, tanh(y/\Delta)\hat{x}$ with $V_0 = 0.4$. To trigger the KHI, we perturb the up or down boundary in three different ways: (1): perturbation of plasma velocity on the boundary as $V_y(x, y) = \epsilon V_0\, sin(kx) exp(-(y - x_b)^2/\Delta^2)$ with the up/down boundary position $x_b = \pm L_y$ and $k = 2\pi/\lambda$. We perturb only one of the boundaries. Here, ϵV_0 defines the amplitude of external perturbation. We set $\epsilon = 0.05, 0.15, 0.3, 0.5$ and $\lambda = 0.040, 0.0625, 0.125, 0.250, 0.450$ for different numerical runs. (2): perturbation of plasma velocity on the boundary in the form $V_y(x, y) = \sum[A_n\, sin(k_n x) + B_n\, cos(k_n x)] exp(-(y - x_b)^2/\Delta^2)$ which is the linear superposition of multiple ($n = 1 : 10$) sinusoidal waves with random amplitudes and wavelengths specified below. (3): perturbation of plasma velocity on the boundary in the form $V_y(x, y) = \epsilon V_0\, exp(-(x - L_x/2)^2/\Delta^2)\, exp(-(y - x_b)^2/\Delta^2)$, which is a velocity perturbation with a single pulse localized at $x = L_x/2$ and $y = x_b$ with $x_b = -L_y$ (down boundary). We emphasize that, any initial perturbation is imposed only on the boundary of plasma, not the interface layer.

The square simulation box size in the $x - y$ plane is $x = [0,\, L_x]$ and $y = [-L_y,\, L_y]$, with dimensionless $L_x = 2L_y = 1.0$. Therefore, the interface layer between two fluids is set at $y = 0$ line parallel to the x axis. The number of grid points is $N_x = N_y = 800$, so the spatial

grid sizes are $\Delta x = \Delta y = 0.00125$. In addition, the CFL condition determines the time step at every integration cycle. Considering the assumption that $\Delta << L_y$, the density and velocity profiles are approximately step functions. This means that for $y < 0$ the velocity is $\mathbf{V}(y < 0) \approx -0.4\hat{\mathbf{x}}$ and $\rho(y < 0) \approx 1.0$, while for $y > 0$ the velocity is $\mathbf{V}(y > 0) \approx +0.4\hat{\mathbf{x}}$ and $\rho(y > 0) \approx 0.5$. Moreover, a uniform magnetic field parallel to the streaming flow is initially imposed in the form $\mathbf{B} = B_0\,\hat{\mathbf{x}}$ with $B_0 = 0.002$. We applied open (outflow) boundary conditions on all boundaries in the x and y directions.

3 SIMULATION RESULTS and DISCUSSION

Considering the initial profiles, parameters, and simulation setup, we now run the 2D MHD PLUTO code to study the externally driven KHI in a magnetized compressible plasma. The main purpose is the study of KHI which is driven by the external perturbation applied on the boundary. Indeed, our simulations can be extended to the case where both up and down boundaries, parallel to the interface layer, are simultaneously perturbed symmetrically or asymmetrically in terms of the perturbation amplitude. However, the general results will be similar. Our results are presented in three subsections according to the type of external perturbation described in Section 2; Forced KHI with a single-wavelength wave (Section 3.1); Forced KHI with a multiple-wavelength wave (Section 3.2); Forced KHI with a single pulse (Section 3.3).

3.1 Forced KHI driven by a single-wavelength wave

First, we perturb perpendicularly the up boundary ($y = +L_y$) with a sinusoidal wave in the form $\mathbf{V}_{pert} = V_y(x, y)\hat{j} = \epsilon V_0\, sin(kx) exp(-(y - L_y)^2/\Delta^2)\hat{j}$ where $k = 2\pi/\lambda$. Here, we run five simulations with $\lambda = 0.040, 0.0625, 0.125, 0.250, 0.450$, and $\epsilon = V_0 = 0.4$. The corresponding wavenumbers are $k = 157.0, 100.48, 50.24, 25.12, 13.96$ respectively. Nevertheless, if the initial perturbation is tangential to the boundary in such a way that there is only a parallel component of velocity, i.e., $V_{pert,x} \neq 0$, $V_{pert,y} = 0$, then the V_y component will also be generated according to the momentum equation of equation (1). However, considering only the perpendicular perturbation is more convenient in our simulations. Figure 1 plots the spatiotemporal variation of the z-component of flow vorticity, $\omega_z = (\nabla \times \mathbf{V})_z$, normalized to $V_0/\Delta y$, in the $x - y$ plane for $\lambda = 0.125 L_x = 0.125$. The initial perturbation in the vorticity imposed on the up boundary is seen in Figure 1(a). The initial velocity perturbation excites magnetoacoustic MHD waves that propagate in the fluid with a local velocity which is determined by both the sound and Alfvén speeds. MHD waves perturb the velocity, density, and pressure of the compressible plasma and the magnetic field everywhere as the wave reaches there. For example, Figure 2 shows the propagation of the perturbed plasma density in the $x - y$ plane.

As the MHD waves arrive at the interface layer, influence the initially stable shear flow with associated perturbations. Note that, when the wave arrives at the interface layer, the amplitude of velocity perturbation is relatively smaller compared with its magnitude on the boundary. For example, in this case, $V_y(t = t_l, y = 0)/\epsilon V_0 = 0.03/0.16 \sim 0.19$. Here, t_l is the time when the wavefront reaches the interface layer. As a result, even with such a weak local perturbation, the KHI is triggered on the interface layer. Figs. 1(b-d) show how a KHI develops fast from a linear regime into a fully nonlinear one, where the vortices grow adequately and merge to produce larger ones. This well-known nonlinear stage of KHI is similar to those results published previously where the initial perturbation is applied on the interface layer. Therefore, the subsequent late-time nonlinear regime of KHI is independent

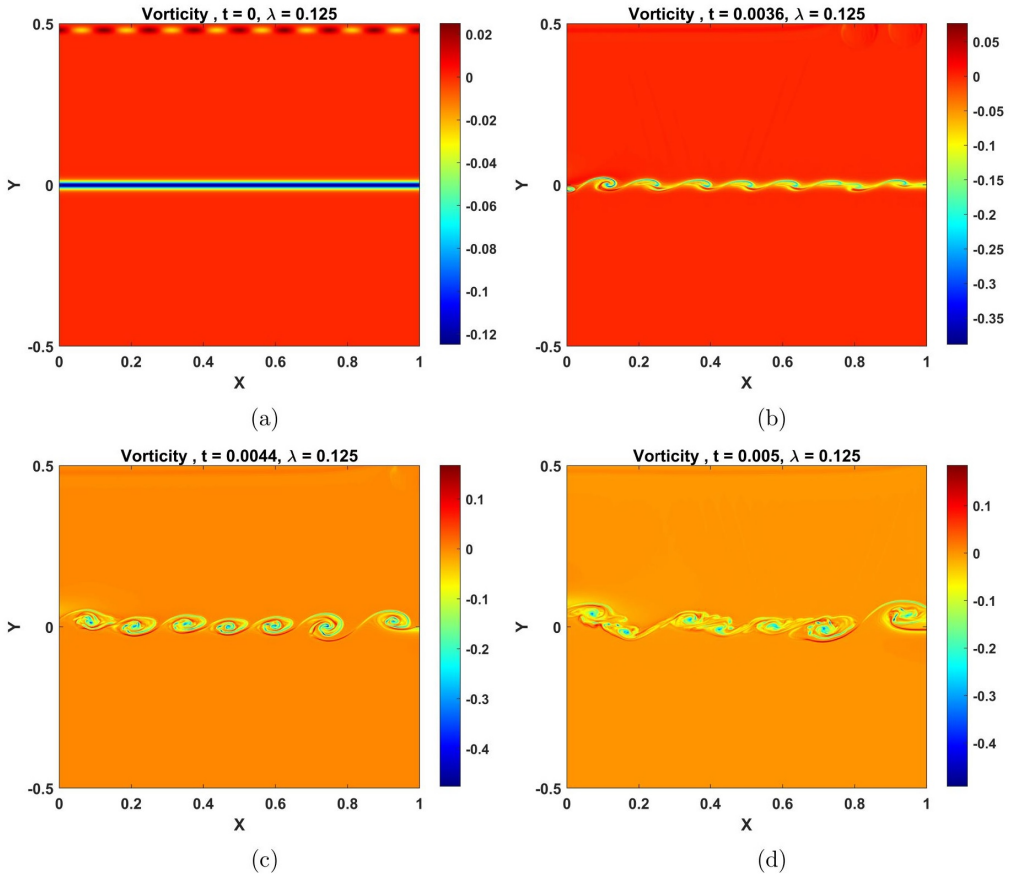

Figure 1: The $z-$ component of flow vorticity on the $x-y$ plane at different times (color online).

of the initial perturbation type and position. So far, it can be concluded that an external perturbation imposed on a boundary of plasma in the form of a sinusoidal wave with a finite wavelength is capable enough to trigger the KHI on the interface layer between two fluids with a shear flow, and it is not necessary to apply an initial perturbation on the interface layer to excite the KHI. Similarly, Figure 3 shows the spatiotemporal variation of magnetic flux contours, ψ, defined by $\mathbf{B} = \nabla \times (\psi \hat{\mathbf{z}})$ for $\lambda = 0.125$. As the KHI develops, initially uniform and straight magnetic field lines are perturbed and rolled up by flow vortices due to the frozen-in-flow condition in a highly conductive plasma, which leads to strong spatial gradients on the boundaries of vortices. The amplification of the magnetic field via the dynamo process occurs mainly on the boundaries of vortices during KHI. To clarify the effect of perturbation wavelength on the KHI, Figure 4 depicts the $z-$component of flow vorticity for four values of wavelength $\lambda = 0.040, 0.125, 0.250, 0.450$ at the same time $t = 0.004$ and amplitude. According to Figure 4, the growth of vortex structures during KHI becomes faster as the perturbation wavelength increases, or equivalently, the wavenumber decreases. Therefore, a perturbation with a larger wavelength is more favorable for driving the KHI. Regarding the effect of perturbation wavelength on the magnetic energy of KHI, Figure 5 shows the time variation of the logarithm of perturbed magnetic energy normalized to the initial magnetic energy, $\Xi \equiv Log(\zeta)$ with $\zeta \equiv [E_{mag}^{(tot)} - E_{mag}^{(0)}]/E_{mag}^{(0)}$, for five different values

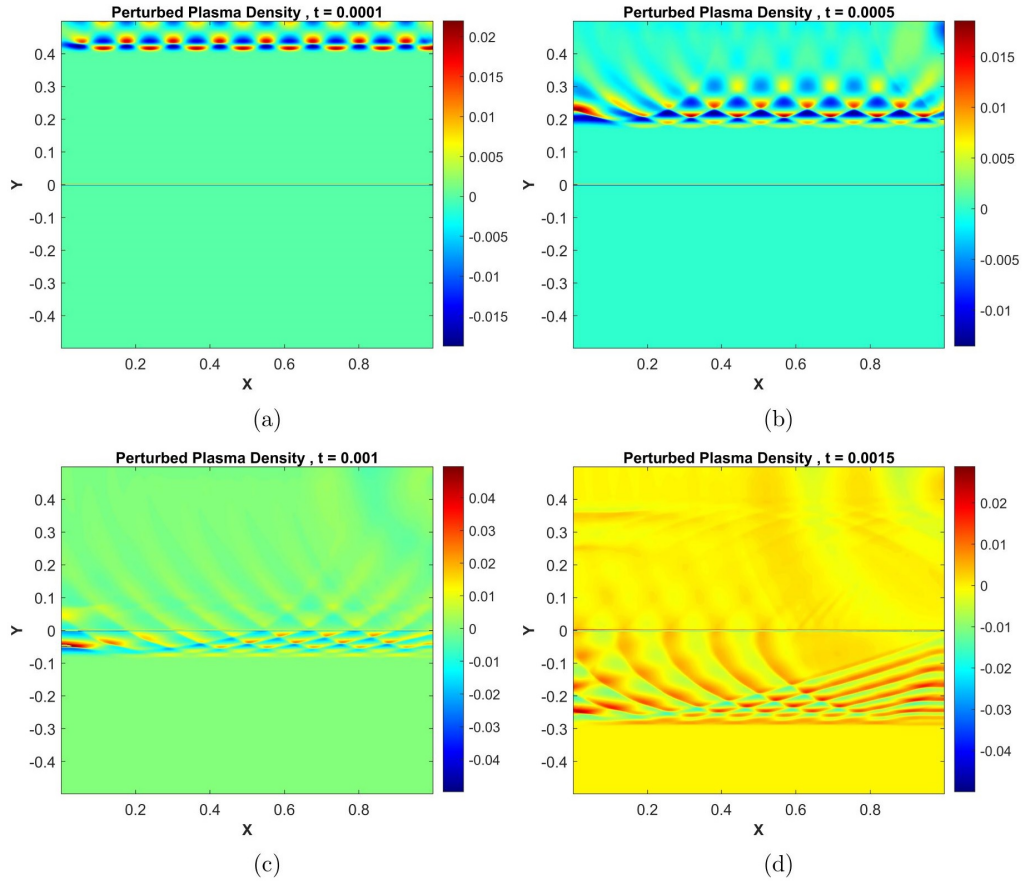

Figure 2: Time variation of the perturbed plasma density at different times (color online).

of perturbation wavelength, λ. As mentioned above, the initial magnetic field for all cases is parallel to the initial flow stream with the magnitude $B_0 = 0.002$. As seen, the growth rate of magnetic energy decreases as the wavelength increases. For example at $t \sim 0.0015$, $\zeta(\lambda = 0.062)/\zeta(\lambda = 0.250) = exp(\Xi(\lambda = 0.062))/exp(\zeta(\Xi = 0.250)) = exp(-1.2)/exp(-4.2) \sim 20$. However, at later times, in the fully nonlinear regime of KHI, magnetic energy is saturated, and reaches a value almost independent of the wavelength magnitude. It seems that the effect of wavelength magnitude on the magnetic energy evolution and the dynamics of vortices are quite different, at least at early times of KHI.

The last point we discuss in this subsection concerns the effect of perturbation amplitude, ϵV_0, on the KHI. Figure 6 presents the time variation of the logarithm of perturbed magnetic energy normalized to the initial magnetic energy, Ξ that is defined above. As expected, the perturbed magnetic energy increases by increasing the amplitude of the perturbation wave. The growth rate of magnetic energy is larger at very early times when the KHI is in the linear stage. However, at later times, it becomes saturated, and therefore, independent of the perturbation amplitude. Moreover, a similar effect is found for the dynamics of vortices. That is, for larger amplitudes, vortices are formed considerably fast.

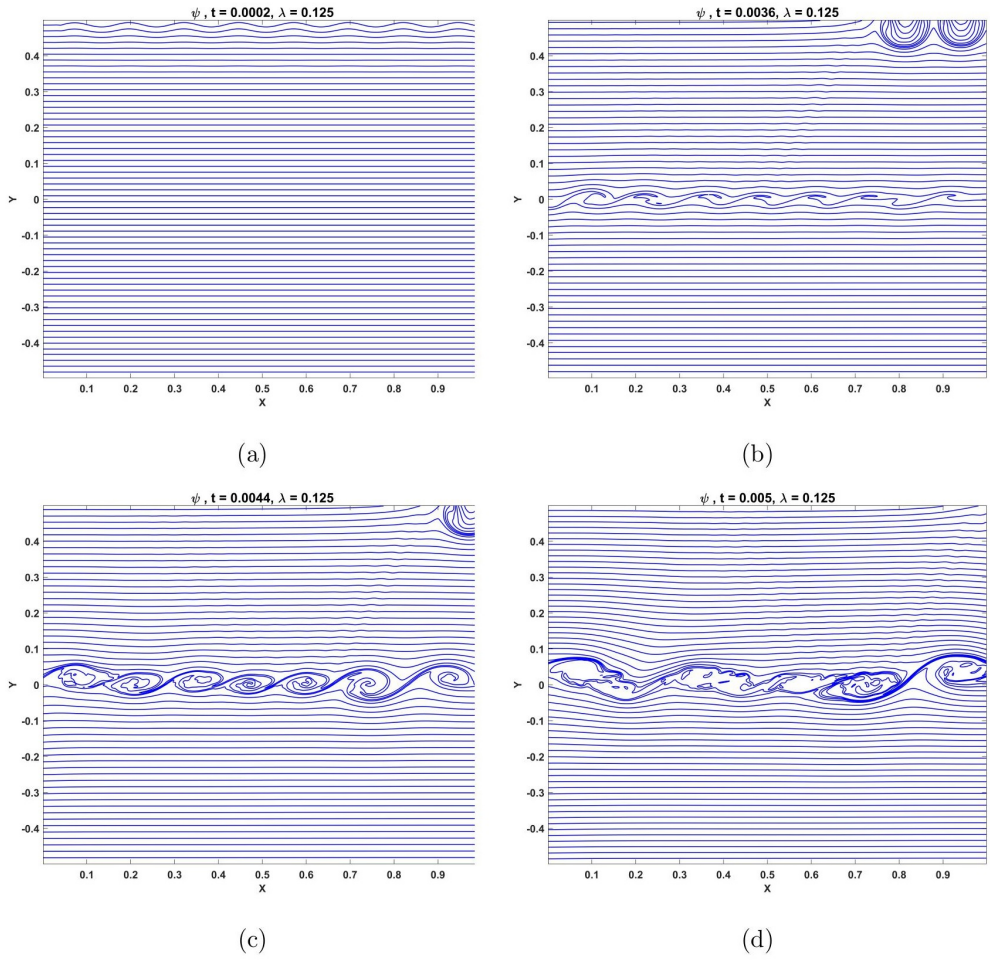

Figure 3: Contours of magnetic flux function, ψ, at different times.

3.2 Forced KHI driven by a multiple-wavelength wave

It is more realistic to consider a complex disturbance of plasma boundaries perturbed simultaneously with multiple modes rather than a single-wavelength wave. Therefore, in this subsection, the upper boundary ($y = +L_y$) is disturbed with a perturbation of perpendicular velocity in the form $V_y(x, y) = \sum_{n=1}^{10}[A_n\, sin(k_n x) + B_n\, cos(k_n x)]exp(-(y - L_y)^2/\Delta^2)$, which is the linear superposition of ten sinusoidal waves with random amplitudes and wavelengths as

$$A_n = [0.1, 0.08, 0.07, 0.06, 0.05, 0.055, 0.066, 0.073, 0.075, 0.081],$$
$$B_n = [0.03, 0.04, 0.05, 0.055, 0.06, 0.051, 0.042, 0.038, 0.032, 0.02],$$
$$k_n = [139.6, 103.0, 50.24, 41.59, 29.90, 25.12, 20.29, 17.44, 14.95, 12.82].$$

We note that the values of A_n and B_n are small in comparison to the amplitudes ϵV_0 considered in the case of single-wavelength wave (Section 3.1). In other words, all modes that are supposed to disturb the boundary are considerably weak. Similar to the single-wavelength mode, here the KHI is also triggered and develops.

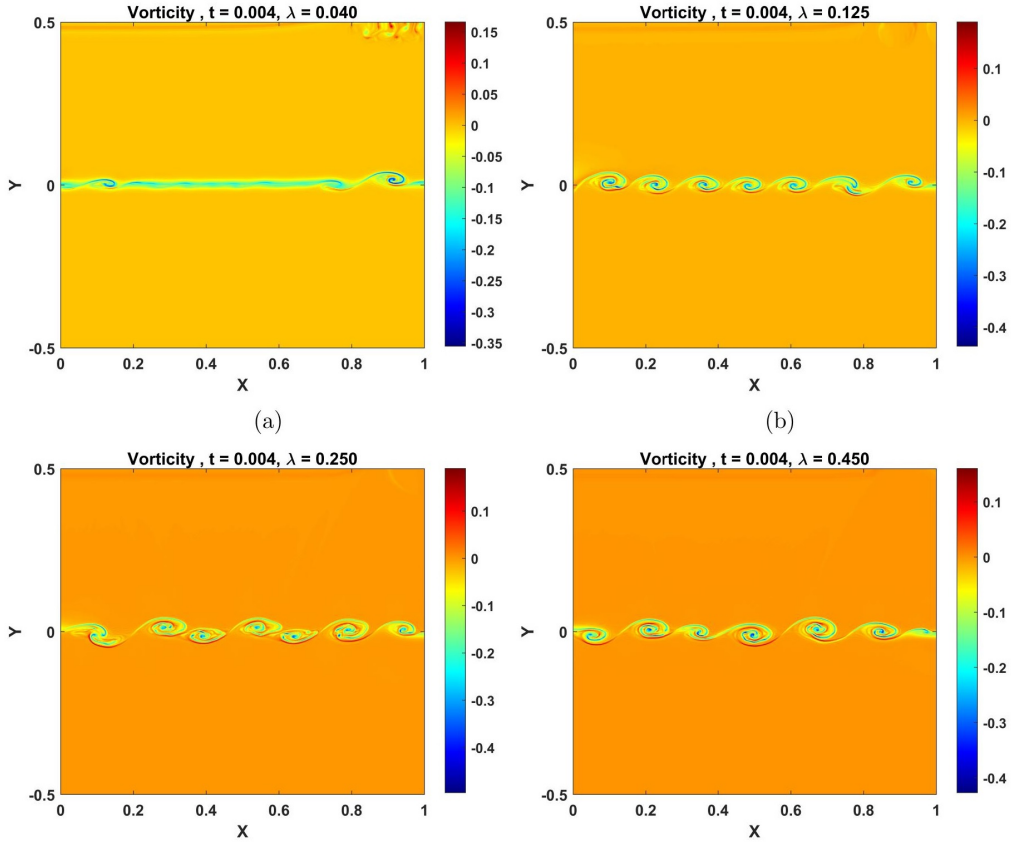

Figure 4: The $z-$ component of flow vorticity on the $x-y$ plane at $t = 0.004$ for four values of wavelength, $\lambda = 0.040$, 0.125, 0.250, 0.450 (color online).

To compare the results with those in the previous subsection, Figure 7 plots the time variation of Ξ for four cases; one of them is the case of multiple-wave perturbation, and the other three are the cases of single-wavelength wave with different wavelengths and amplitudes as specified in Figure 7. In terms of the magnetic energy amplification, obviously, the effect of multiple-wave perturbation is approximately similar to the case of single-wave perturbation with a strong amplitude $\epsilon = 0.5$. However, there is a significant difference with the other two cases of smaller amplitude $\epsilon = 0.3$. Generally speaking, as far as the temporal evolution of perturbed magnetic energy is concerned, the effect of multiple waves with relatively small amplitudes is similar to the effect of a single wavelength wave with a large amplitude. With these set of values for A_n and B_n, the growth of KH vortices is, respectively, slower and faster compared to the cases of a single-wavelength mode with the amplitude of $\epsilon V_0 = 0.5 \times 0.4 = 0.2$ and $\epsilon V_0 = 0.15 \times 0.4 = 0.06$. Applying multiple waves each of them has an amplitude comparable to or greater than the values assumed in the previous subsection, definitely will result in a drastic and fast forced KHI.

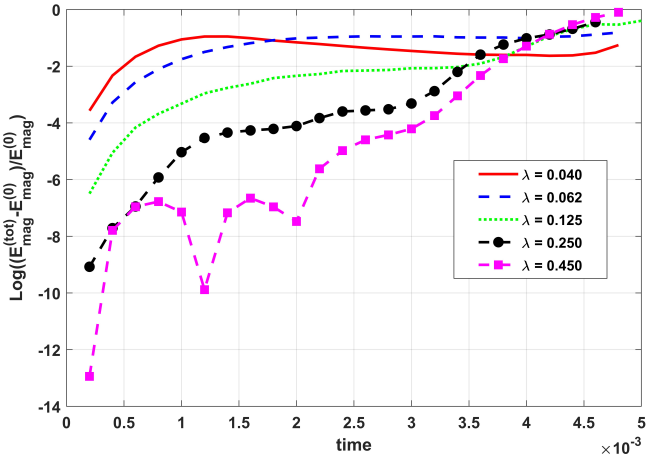

Figure 5: Time variation of the logarithm of perturbed magnetic energy normalized to the initial magnetic energy, Ξ, for five different values of perturbation wavelength (color online).

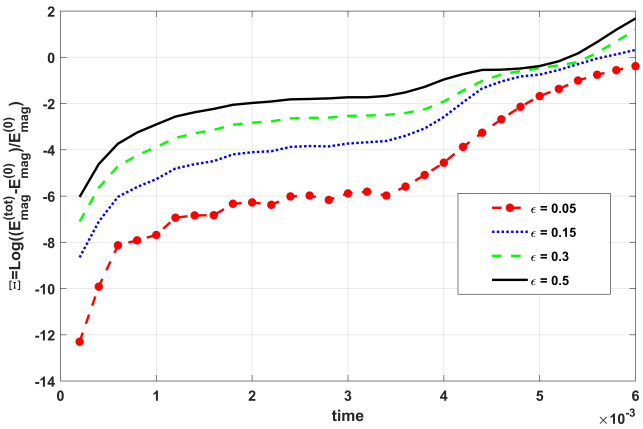

Figure 6: Time variation of the logarithm of perturbed magnetic energy normalized to the initial magnetic energy, Ξ, for four different values of perturbation amplitude (color online).

3.3 Forced KHI driven by a single pulse

The third scenario in our study of forced KHI is disturbance of the lower boundary ($x_b = -L_y$) with a single velocity pulse as

$$V_y(x,y) = \epsilon V_0\, exp(-(x - L_x/2)^2/\Delta^2)\, exp(-(y + L_y)^2/\Delta^2),$$

with a small amplitude $\epsilon V_0 = 0.04$. The pulse is spatially localized at $x = L_x/2$ and $y = -L_y/2$ with a half-width of $\Delta = 0.01$ in each direction. The main question to answer is whether a weak velocity pulse that is highly localized on the boundary can drive the KHI throughout the interface layer with a shear flow.

Figure 8 displays the temporal evolution of the perturbed plasma pressure. As the corresponding perturbation propagates radially away from the initial position in the $x - y$

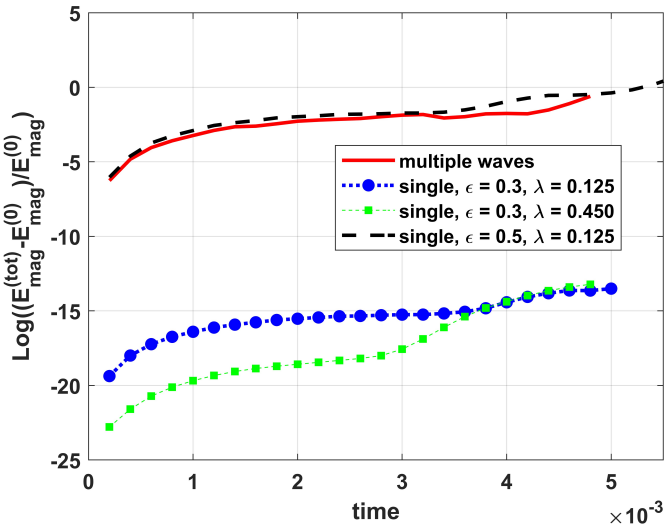

Figure 7: Temporal variation of Ξ for four cases; a multiple-wavelength case and three single-wavelength ones.

plane, its left side ($x < 0.5$) is convected to the left boundary accompanied by the plasma flow and outflows from the left boundary which is set to be open. As the pulse arrives at the interface layer, a fraction of the pulse is reflected and a larger fraction transits into the upper fluid. At the late times of simulation (see Figure 8(e)) irregular perturbations attributed to the KHI are excited on the interface layer that grows in amplitude, with a wavelength $\lambda \sim 0.143$, Figure 8(f). The excitation and subsequent growth of KHI can be seen clearly in the corresponding images of flow vorticity in Figure 9. It can be inferred that even a weak single velocity pulse deeply localized on a boundary can lead to the formation of KHI. The last but not the least point to mention is that, the results of numerical runs with a magnetic pulse in the form

$$B_y(x, y) = \epsilon_b B_0 \, exp(-(x - L_x/2)^2/\Delta^2) \, exp(-(y + L_y)^2/\Delta^2),$$

shows that, the KHI can be again triggered. Since the results are similar to the case of velocity pulse, we do not report the corresponding graphs here. In fact, in a collisionless (zero-resistivity) plasma due to the coupling between the plasma velocity and the magnetic field, the excitation of each of these leads to the similar excitation of the other one.

4 Summary and Conclusion

Two-dimensional MHD numerical simulations are carried out to study the externally driven KHI in a compressible magnetized plasma with a shear flow on the interface layer. The initial magnetic field is parallel to the streaming flows and the fluids are assumed highly conductive plasmas with zero resistivity. To trigger the KHI on the interface layer, we disturbed the up or down boundary with a component of plasma velocity that is perpendicular to the streaming flows. It is worthy of note that, any sufficient and appropriate perturbation of plasma velocity, density, pressure, or the magnetic field results in the excitation of MHD waves that propagate away from the boundary towards the interface layer. Even a disturbance of a

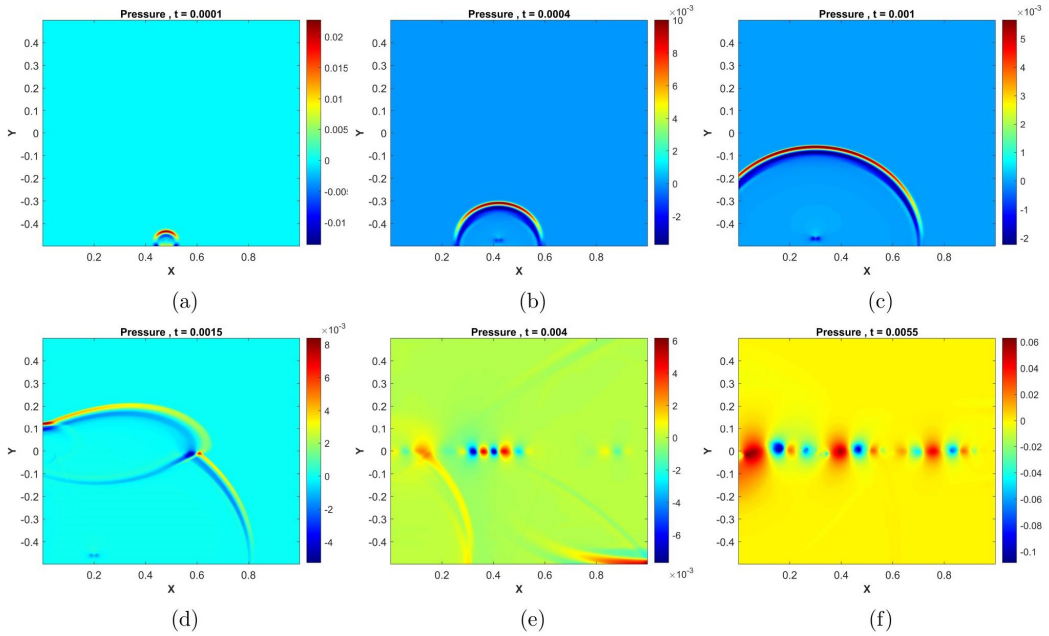

Figure 8: The perturbed plasma pressure on the $x-y$ plane at six different times (color online).

boundary with an appropriate parallel component of velocity, i.e., tangential perturbation, can lead to the excitation of KHI. As the wave perturbations arrive at the initially stable shear flow, the noises will grow in time. Eventually, the interface layer becomes unstable to the KHI and the associated vortices are gradually formed. As the structures of vortices develop, the instability transits into a nonlinear regime and then into a turbulent phase where secondary giant vortices appear by merging with large vortices.

In our simulations, the boundary disturbance has been carried out in three ways: First, we disturbed the upper boundary with the perturbation of the perpendicular component of plasma velocity in the form of a sinusoidal wave with a specified amplitude and wavelength. Note that, the boundary perturbations in all three types take place only one time, initially at $t = 0$. The results showed that a sinusoidal perturbation of velocity with a finite wavelength can trigger the KHI on the boundary. The formation of KH vortices is faster for a wave with a larger wavelength. However, the amplification of magnetic energy is stronger when the wavelength is smaller. Nevertheless, the temporal evolution of both the KH vortices and the magnetic energy appears to be saturated eventually, and therefore independent of the wavelength magnitude in the late times, when the instability is in the fully nonlinear regime. In addition, a strong perturbation with a larger amplitude results in a faster KHI (i.e., high growth rate).

As a second scenario of external disturbance which is more realistic, we perturbed the upper boundary with a complex mode which is the linear superposition of multiple sinusoidal waves with random amplitudes and wavelengths that are applied on the boundary simultaneously. We considered small amplitudes and very short wavelengths. We found that the initial formation of KH vortices on the interface layer is relatively irregular regarding their appearance location and topology. This is due to the initial profile of the perturbation wave which is the superposition of ten sinusoidal waves with different amplitudes and

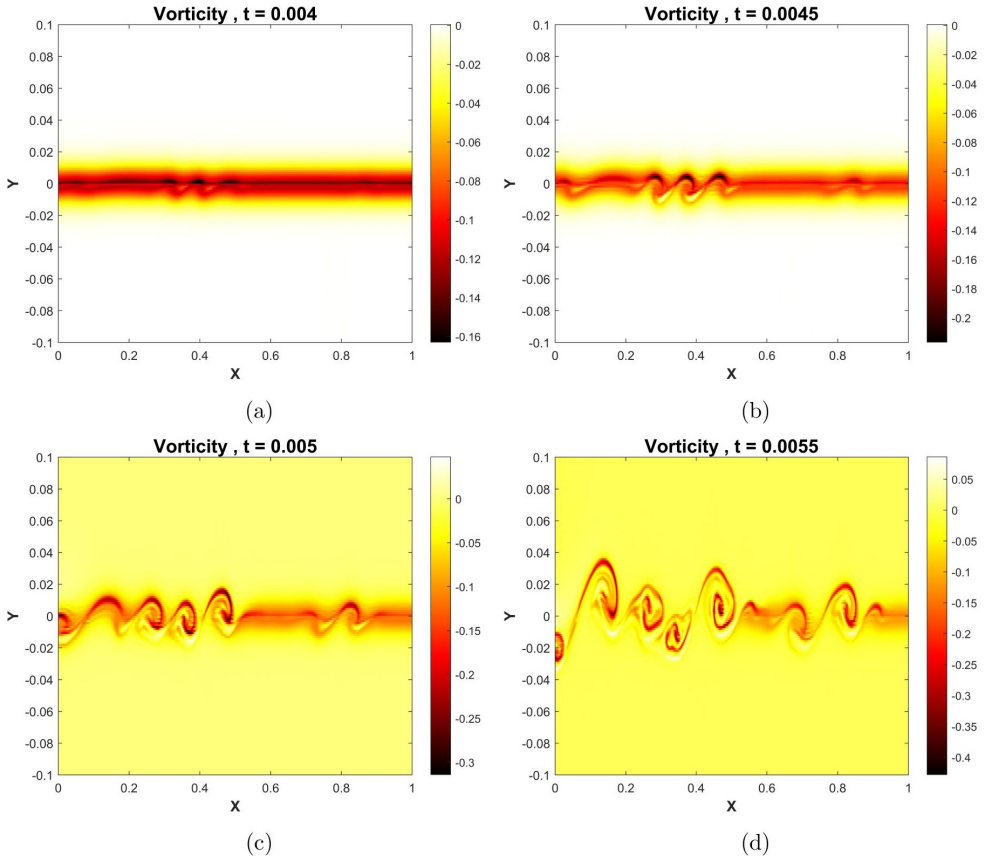

Figure 9: The z-component of flow vorticity on the $x-y$ plane at four different times (color online).

wavelengths. The effect of this type of perturbation on the KHI is comparable to the effect of a single sinusoidal wave with a larger amplitude.

The last way of disturbance was to apply a single velocity pulse being highly localized on a narrow region on the boundary. The pulse is localized in the middle of the $x-$ direction (parallel to the interface layer) in the vicinity of the down boundary in order to affect symmetrically both the left and right sides of the interface layer. As the pulse propagates radially in the fluid, it is also pushed towards the left boundary due to the flow stream from the right to the left below the interface layer. As a result, some part of the pulse leaves the fluid through the open boundary, and therefore, the symmetry of the propagating pulse is broken. As the pulse arrives at the interface layer where the density is different above and below, then a fraction of the pulse is reflected and another fraction transits into the other fluid. Eventually, perturbations affect irregularly the interface layer with a shear flow, and irregular KH vortices are formed there. This means that even a weak velocity pulse imposed on the boundary can bring drastic effects to the structure of the initially stable interface layer by driving KHI. We also found that a localized pulse of magnetic field imposed on the boundary leads to similar dynamics of KHI that were observed in the case of a velocity pulse.

Three final points to mention: first, we emphasize that, in the absence of any external perturbation, there will be no sign of KHI on the interface layer which is initially free of

internal perturbations. Under these conditions, the KHI was not observed even at very long times of simulation.

Second, the externally driven KHI is important when the interface layer with a shear flow is free of any internal perturbation or the internal perturbation is very weak to trigger the KHI, particularly, when the shear flow is weak. In the space and astrophysical plasmas, the length of the possible interface layer is large. Therefore, it is highly likely that the external boundaries of plasmas are easily disturbed by a single pulse or a wave of plasma velocity or magnetic field perturbation. Since the space plasmas are relatively less dense, the propagation velocity of MHD waves is relatively larger. This means that any perturbation on the external boundary can reach the interface layer very quickly.

Third: our study is the extension of the idea presented by the "Taylor problem" of the forced magnetic reconnection (Hahm and Kulsrud, 1985) to the KHI. According to this theory, the onset of magnetic field line reconnection within the current layer is due to the boundary disturbance of a highly conductive plasma embedded in a magnetic field that changes its direction in a narrow non-ideal MHD region, called the current sheet. It was interesting to extend this general idea to the KHI and to study whether the KHI can be triggered by a perturbation imposed on the boundary. The main and general conclusion is that the external disturbances imposed on the boundaries as the perturbations of velocity, density, pressure, or magnetic field can trigger the KHI on the interface layer. However, the exact and detailed dynamics such as the topology of KH vortices, the growth rate of instability and energies depend on the way of disturbance and its associated parameters.

Acknowledgements

The author is very thankful to the Pluto code development team for making the code accessible for our simulations.

Authors' Contributions

The author contributed to data analysis, drafting, and revising of the paper and agreed to be responsible for all aspects of this work.

Data Availability

The raw data supporting the conclusions of this article will be made available by the authors, without undue reservation.

Conflicts of Interest

The author declares that there is no conflict of interest.

Ethical Considerations

The author has diligently addressed ethical concerns, such as informed consent, plagiarism, data fabrication, misconduct, falsification, double publication, redundancy, submission, and other related matters.

Funding

This research did not receive any grant from funding agencies in the public, commercial, or non profit sectors.

References

[1] Von Helmholtz H., 1868, Monatsberichte der Königlichen Preussis-che Akademie des Wissenschaften zu Berlin 23, 215.

[2] Kelvin L., 1871, Hydrokinetic solutions and observations, PMag. 42, 362.

[3] Chandrasekhar S., 1961, Hydrodynamic and Hydromagnetic Stability, Oxford: Clarendon.

[4] Hasegawa H., Sonnerup B., Dunlop M., Balogh A., Haaland S., & et al., 2004a, Ann. Geophys., 22, 1251.

[5] Hasegawa H., Fujimoto M., Phan T.-D., Rème H., Balogh A., Dunlop M.W., & et al., 2004b, Nature, 430, 755.

[6] Nykyri K., Otto A., Lavraud B., Mouikis C., Kistler L. M., Balogh A., & Rème H., 2006, Ann. Geophys., 24, 2619.

[7] Nykyri K., 2024, "On the importance of the Kelvin-Helmholtz Instability on magnetospheric and solar wind dynamics during high magnetic shear." Geophy. Res. Lett. 51, e2024GL108605.

[8] Chaston C. C., Wilber M., Mozer F. S., Fujimoto M., Goldstein M. L., & et al., Phys. Rev. Lett. 99, 175004.

[9] Johnson J. R., Wing S., & Delamere P. A., 2014, Space Sci. Rev. 184, 1.

[10] Kotsarenko N., Lizunov G., & Churyumov K., 1990, SvA Lett. 16, 113.

[11] Bucciantini N., & Del Zanna L., 2006, A&A 454, 393.

[12] Boccardi B., Krichbaum T. P., Bach U., Mertens F., Ros E., Alef W. & Zensus J. A., 2016, A&A 585, A33.

[13] Walker R. C., Hardee P. E., Davies F. B., Ly C., & Junor W., 2018, ApJ. 855, 128.

[14] Chow A., Davelaar J., Rowan M. E. & Sironi L., 2023, ApJL 951, L23.

[15] Ryutova, M., Berger T., Frank Z., Tarbell T. & Title A., 2010, Sol. Phys. 267, 75.

[16] Foullon C., Verwichte E., Nakariakov V. M., Nykyri K., & Farrugia C. J., 2011, ApJL, 729, L8.

[17] Zhelyazkov I., Zaqarashvili T. V., & Chandra R., 2015, A&A 574, A55.

[18] Kieokaew, R., Lavraud B., Yang Y., Matthaeus W. H., Ruffolo D., Stawarz J. E. & et al., 2021, A&A 656, A12.

[19] Ofman L. & Thompson B. J., 2011, ApJL, 734, L11.

[20] Zhelyazkov I., & Chandra R., 2020, Kelvin-Helmholtz Instability in Solar Atmospheric Jets, World Scientific Publication.

[21] Hahm, T. S., & Kulsrud, R. M., 1985, Phys. Fluids, 28, 2412.

[22] Fitzpatrick, R., 2004, Phys. Plasmas, 11, 937.

[23] Hosseinpour M., & Vekstein G. 2008, Phys. Plasmas, 15, 022904.

[24] Mignone A, Bodo G., Massaglia S., Matsakos T., Tesileanu O., Zanni C., & Ferrari A., 2007, ApJS. 170, 228.